Economic Modelling 158 (2026) 107523

Contents lists available at ScienceDirect

Economic Modelling

journal homepage: www.journals.elsevier.com/economic-modelling

Climate policy uncertainty and macroeconomic dynamics: Financial amplification and state-dependent effects

Facundo Luna Mallea[1]

Economics Department, Rutgers University, New Brunswick, United States

ARTICLE INFO

Dataset link: Climate Policy Uncertainty and Macroeconomic Dynamics: Financial Amplification and State-Dependent Effects (Original data)

Keywords:
Transition risk
Uncertainty
Volatility
Climate policy
Local projections
DSGE

ABSTRACT

Climate policy uncertainty (CPU) poses growing risks to macroeconomic stability, yet its transmission mechanisms remain understood. While the literature has examined general uncertainty, the state-dependent effects of transition risk through the financial system are underexplored. Using U.S. local projections and a two-sector New Keynesian model, this paper examines how CPU shocks propagate across the business cycle. I find that CPU shocks significantly contract investment and credit during economic expansions, whereas their effects are statistically muted during recessions. These dynamics are driven by a brown collateral channel, where uncertainty about the future value of carbon-intensive assets triggers a financial accelerator mechanism. The findings highlight that transition risk operates as a systemic financial shock, suggesting that macro-prudential frameworks must account for the volatility of brown asset valuations.

1. Introduction

Climate change presents growing macroeconomic and financial risks, prompting governments to adopt policies aimed at steering economies toward sustainable development. While recent studies highlight the macroeconomic costs of physical risks such as temperature shocks (Bilal and Känzig, 2024) or natural disasters (Paudel, 2025), this paper isolates the financial risks stemming from the policy transition itself. Crucially, the pace, scope, and credibility of these policies remain highly volatile. This ambiguity, referred to as Climate Policy Uncertainty (CPU), has emerged as a destabilizing force that impacts investment decisions and asset prices (NGFS, 2024). CPU encompasses uncertainty regarding the timing, stringency, and implementation of regulations — such as carbon taxes or subsidies — as well as technological and political outcomes (Monasterolo et al., 2024). While recent work shows that CPU increases financial volatility and dampens investment (Palikhe et al., 2024), its transmission mechanisms through the financial system and its state-dependent effects remain underexplored.

This paper examines the macroeconomic and financial implications of CPU through a two-pronged empirical and theoretical approach. Empirically, I estimate local projections using monthly U.S. data from 1990–2020. I construct a composite CPU measure via principal component analysis, combining the Environmental Policy Uncertainty index (Palikhe et al., 2024) with the Equity Market Volatility Tracker for Energy and Environmental Regulation (Baker et al., 2026), capturing both regulatory and market-based dimensions of risk.

The empirical analysis yields three core findings. First, CPU shocks are contractionary: a one-standard-deviation innovation reduces investment by 1%, lowers industrial production, and tightens business lending by 1.5%. Second, these effects are highly state-dependent. CPU shocks generate large contractions during economic expansions but have statistically negligible effects during recessions—a pattern confirmed by joint F-tests. This contrasts with standard uncertainty measures like the VIX, which typically amplify during downturns (Bloom, 2009). Third, CPU induces sectoral reallocation: fossil fuel production falls persistently while renewable output expands. This compositional shift is concentrated in expansions, suggesting that the transmission mechanism relies on firms' capacity to redirect investment.

To rationalize these patterns, I develop a two-sector New Keynesian DSGE model featuring green and brown production, financial frictions à la Gertler and Karadi (2011), and Epstein–Zin preferences. I model CPU through two potential channels: volatility in the carbon tax rate versus volatility in the quality of brown capital. Calibrating the volatility processes to the empirical CPU index, I find that only the capital quality channel can reproduce the data.

The intuition relies on the distinction between "flow risk" and "stock risk." Carbon tax volatility represents flow risk: it affects the variance of future profits but has a dampened impact on present

E-mail address: facundo.luna@rutgers.edu.

[1] I am grateful to the editor, Prof. Sushanta K. Mallick, and two anonymous reviewers of Economic Modeling for their constructive comments and suggestions, which have substantially improved this paper. Any remaining errors are my own.

https://doi.org/10.1016/j.econmod.2026.107523
Received 12 October 2025; Received in revised form 30 January 2026; Accepted 30 January 2026
Available online 10 February 2026

asset values due to discounting. In contrast, capital quality volatility represents stock risk: it directly impairs the pledgeable value of brown assets. Because brown capital serves as collateral for the banking sector, this devaluation tightens the leverage constraint of financial intermediaries, generating a credit contraction that spills over to the aggregate economy. This mechanism explains why CPU shocks produce a broad downturn rather than a smooth sectoral rotation, and why the effects are most potent during expansions when collateral constraints bind and credit is actively flowing.

This paper contributes to the literature by identifying the unique signature of climate policy risk relative to general uncertainty (Basu and Bundick, 2017; Gilchrist et al., 2014). I show that CPU transmits primarily through financial frictions rather than operating costs alone, extending recent work on environmental uncertainty (Noailly et al., 2022, 2024). By distinguishing between tax volatility and capital quality volatility, the model provides a structural interpretation of transition risk as a shock to the financial valuation of brown assets (Ferrari and Nispi Landi, 2024; Carattini et al., 2023).

2. Literature review

This paper connects three strands of literature: general macroeconomic uncertainty, economic policy uncertainty, and the emerging field of climate finance.

The first strand is the extensive literature that establishes uncertainty as a driver of fluctuations. Bernanke (1983) and Pindyck (1986) formalized the "real options" channel, where uncertainty delays irreversible investment. Modern macro-finance models emphasize that financial frictions amplify these shocks by widening credit spreads (Gilchrist et al., 2014) or through demand channels where nominal rigidities convert precautionary savings into output losses (Basu and Bundick, 2017). Bloom et al. (2018) and Tenreyro and Thwaites (2016) document that standard uncertainty shocks are typically more damaging during recessions. My results highlight that CPU behaves differently, exerting its strongest effects during expansions when the capacity for sectoral reallocation is high.

Additionally, this work builds on measures of policy-specific uncertainty. Baker et al. (2016) developed the Economic Policy Uncertainty (EPU) index, linking policy ambiguity to investment declines and recessions. Subsequent research extends this to trade (Caldara et al., 2020) and geopolitical risk (Caldara and Iacoviello, 2022). Recent studies show that climate policy uncertainty interacts with these broader risks; Eissa et al. (2024) finds spillovers between CPU, geopolitical risk, and oil volatility, while Tan et al. (2024) demonstrates that hedging strategies against CPU vary nonlinearly with market conditions.

Finally, a rapidly growing literature focuses specifically on environmental policy uncertainty. Palikhe et al. (2024) and Noailly et al. (2024) construct text-based indices for the U.S., finding that high uncertainty depresses brown-sector investment and employment. Noailly et al. (2022) shows that this uncertainty also hampers venture capital funding for green startups. Cross-country evidence from Berestycki et al. (2022) confirms these negative investment effects, while Ren et al. (2022) finds CPU constrains R&D in Chinese firms. On the financing side, Hoang et al. (2026) suggests that green lending can mitigate some transition risks, and Adetutu et al. (2023) highlights the role of regulatory stringency.

Existing studies confirm that CPU drives sectoral reallocation. However, they largely abstract from the aggregate financial transmission mechanism. This paper fills that gap by modeling CPU as a shock to the collateral value of brown assets. By integrating the financial accelerator mechanism (Gertler and Karadi, 2011) with environmental macroeconomics (Diluiso et al., 2021; Fried et al., 2021; Khalil and Strobel, 2023; Huang and Punzi, 2024), I show that transition risk acts as a systemic financial shock, explaining the aggregate contraction and state-dependence observed in the data.

3. Data and methodology

3.1. Data

This paper uses monthly U.S. macroeconomic and financial data from January 1990 to December 2020 obtained from the Federal Reserve Economic Data (FRED) database. The baseline variables include industrial production, personal consumption expenditures (PCE), the PCE price index (inflation), the unemployment rate, the effective federal funds rate, credit to nonfinancial firms, and gross fixed capital formation as a proxy for investment. U.S. CO_2 emissions are included to capture the environmental response to shocks.

To capture climate and environmental policy uncertainty, I use two independent news-based indices. The first is the Environmental Policy Uncertainty (EnvPU) index compiled by Palikhe et al. (2024). This index measures uncertainty surrounding U.S. environmental regulation using a text-based approach applied to over 300 million newspaper articles from 1985 to 2020. The index identifies articles that simultaneously reference economic or policy-related terms, general uncertainty keywords, and a curated list of 31 environment-specific terms such as "carbon tax" or "EPA regulation." The monthly count of such articles is normalized to create a time-series index that reflects perceived regulatory uncertainty. This method builds on the framework of Baker et al. (2016) but is tailored to the environmental policy context. The authors show that the index correlates with major regulatory events and has predictive power for firm-level investment and employment responses, particularly in pollution-intensive sectors.

I also use the "Equity Market Volatility Tracker: Energy and Environmental Regulation" index (VIX-EER), which is a specialized index developed by Baker et al. (2026).[2] It measures the extent to which equity market volatility is associated with news related to energy and environmental regulation. This tracker is part of a broader set of indices that analyze how different policy areas influence market volatility. The EMV Tracker counts monthly articles from 11 major U.S. newspapers (e.g., New York Times, Wall Street Journal, Chicago Tribune) that contain terms related to **E**conomy, **M**arket and **V**olatility. The raw counts of EMV articles are scaled by the total number of articles in the same newspaper and month to account for variations in news volume. The resulting series is multiplicatively rescaled to match the mean value of the CBOE Volatility Index (VIX), ensuring the EMV Tracker moves with the VIX and the realized volatility of S&P 500 returns.

While both indices capture climate-related policy uncertainty, EnvPU reflects broad uncertainty surrounding environmental policymaking, whereas EMV-EER isolates the component of that uncertainty that is salient for equity markets and investment decisions; accordingly, their use is complementary rather than substitutable.

Therefore, to capture a unified measure of climate and environmental policy uncertainty, I construct a composite index by combining the Environmental Policy Uncertainty (EnvPU) index and the Equity Market Volatility Tracker for Energy and Environmental Regulation (EMV-EER). Both indices are derived from text-based analyses of major U.S. newspapers, with EnvPU focusing on regulatory uncertainty related to environmental issues and EMV-EER capturing volatility in equity markets linked to news about energy and environmental policies. Using principal component analysis (PCA), I extract the first principal component from these two series, which represents the largest shared variation and effectively summarizes their common informational content.

The principal component of EMV-EER and EnvPU captures the common component of climate policy uncertainty that is both institutionally salient and financially relevant, filtering out index-specific noise and isolating a shared latent factor. As a result, the composite index provides a parsimonious proxy for systemic uncertainty surrounding the climate transition, reflecting both regulatory and market-based dimensions of climate policy risk.

[2] Available at https://fred.stlouisfed.org/series/EMVENRGYENVREG/.

3.2. Methodology

To estimate the dynamic effects of climate and environmental policy uncertainty on key macroeconomic and financial variables, I employ the local projection (LP) method proposed by Jordà (2005). Local projections offer distinct advantages over vector autoregressions (VARs) in this context. Unlike VARs, which require accurate specification of the joint dynamics of all variables, LPs estimate impulse response functions (IRFs) horizon by horizon, imposing minimal assumptions about the underlying data-generating process (DGP). This makes LPs more robust to misspecification, particularly when structural breaks or complex dynamics are present (Ramey, 2018; Plagborg-Møller and Wolf, 2021). Additionally, LPs facilitate flexible extensions, such as state-dependent or nonlinear models, which are well-suited to capture potential asymmetries in responses to climate policy uncertainty (Tenreyro and Thwaites, 2016; Barnichon and Brownlees, 2019).

The LP framework estimates IRFs by regressing the future value of an outcome variable on a climate policy uncertainty (CPU) shock and a set of controls. For each horizon $h = 0, 1, \dots, 60$, I estimate the following equation:

$$y_{t+h} = \alpha_h + \beta_h \cdot \text{CPU Shock}_t + \sum_{\tau=1}^{p} \phi_{\tau,h} y_{t-\tau} + \sum_{\tau=1}^{p} \sigma_{\tau,h} \text{CPU}_{t-\tau} + \sum_{\tau=1}^{p} \lambda_{\tau,h} Z_{t-\tau} + \varepsilon_{t+h}, \quad (1)$$

where y_{t+h} represents the different macroeconomic or financial variables (e.g., industrial production, investment, emissions, S&P 500 index) at time $t + h$, and CPU Shock$_t$ is the standardized shock for each CPU index at time t. The coefficient β_h represents the IRF at horizon h to a one-standard-deviation CPU shock. The vector Z_t includes lags of control variables, specifically the U.S. Economic Policy Uncertainty index (Baker et al., 2016), changes in the WTI oil prices, and the VIX index, to isolate CPU effects from broader economic and financial uncertainty. Additionally, I incorporate a dummy indicator for the NBER recession period to account for aggregate business cycle fluctuations. The number of lags p is selected using the Akaike Information Criterion (AIC) based on an auxiliary VAR, ensuring robust control for DGP dynamics (Olea et al., 2025). Standard errors are corrected for heteroskedasticity using robust estimators, and IRFs are reported in percent deviations from baseline with 90% confidence intervals.

As a robustness check, I also estimate an instrumental variable (IV) LP model

$$y_{t+h} = \alpha_h + \beta_h \cdot \text{CPU}_t + \sum_{\tau=1}^{p} \phi_{\tau,h} y_{t-\tau} + \sum_{\tau=1}^{p} \lambda_{\tau,h} Z_{t-\tau} + \varepsilon_{t+h}, \quad (2)$$

where CPU$_t$ is instrumented by CPU Shock$_t$. The IV approach ensures that the estimated IRFs capture the causal effect of exogenous CPU innovations, controlling for feedback from macroeconomic conditions (Olea et al., 2025).

Estimating in levels (rather than first differences) preserves the economically meaningful object—level responses that are directly comparable to the model-generated log deviations, while the lag controls absorb persistence and deliver robustness to mild misspecification. This practice is consistent with the LP–VAR equivalence results of Plagborg-Møller and Wolf (2021), who show that (with unrestricted lags) LPs and VARs target the same population IRFs, and with applied macro work on uncertainty shocks that reports level IRFs (Bloom, 2009; Basu and Bundick, 2017).

The CPU shock is constructed to isolate exogenous innovations in policy uncertainty, following standard practices in the uncertainty literature (Jurado et al., 2015). The CPU indices are news-based measures derived from the frequency of articles in major U.S. newspapers referencing climate policy and uncertainty. To extract unanticipated shocks, I estimate an autoregressive model with data-driven lag selection:

$$\text{CPU}_t = \alpha + \sum_{\tau=1}^{p} \phi_\tau \text{CPU}_{t-\tau} + \sum_{\tau=1}^{p} \gamma_\tau W_{t-\tau} + \varepsilon_t^{\text{CPU}}, \quad (3)$$

where W_t includes lagged macroeconomic controls (e.g., personal consumption expenditures, unemployment rate, core inflation, investment, industrial production, S&P 500, business loans, federal funds rate, WTI prices) and broad uncertainty measures (VIX and USEPU) in levels or first differences based on stationarity tests (Dickey–Fuller). The lag length p is selected via AIC from an auxiliary VAR, ensuring all relevant dynamics are captured (Olea et al., 2025). The residuals $\varepsilon_t^{\text{CPU}}$ represent the unexpected component of CPU, and are then standardized.

The resulting shock series (Fig. 1) displays distinct spikes that align with major environmental policy events, reflecting heightened periods of perceived regulatory uncertainty. The largest peaks correspond to the 1986 renewal of the Clean Water Act, the first official Earth Day in 1990, and the 1993 proposal of the BTU tax. A significant increase in uncertainty is also observed around the transition to the George W. Bush administration in January 2001, which marked a shift in climate policy direction, including the rejection of the Kyoto Protocol as "not acceptable" to the administration or Congress. Additional spikes occur during the 2010 BP oil spill and the 2011 rollback of air quality standards. The spike in 2013 is due to Obama's Climate Action Plan, which represented a significant shift toward using executive authority and EPA regulations for climate policy after cap-and-trade failed in Congress. The indices do not show substantial responses to international agreements with limited domestic enforcement, such as the 2015 adoption and the 2017 U.S. withdrawal from the Paris Agreement, which lacked Congressional ratification and had little immediate impact on U.S. policy. The late 2010s experienced continued elevated uncertainty amid the Green New Deal debate, growing climate activism, and the announcement of the European Green Deal. This pattern confirms that the shock measures capture meaningful variation in climate policy uncertainty tied to identifiable political and regulatory events.

Additionally, I estimate the shocks by estimating the stochastic volatility parameters using a GARCH procedure to discipline the uncertainty shock dynamics in the theoretical model. Specifically, I estimate an AR(1)-GARCH(1,1) model on the CPU index with macroeconomic controls and broad uncertainty measures in the mean equation. This specification isolates the CPU-specific component of volatility after controlling for general macroeconomic conditions and broader uncertainty measures.

To examine whether CPU shocks propagate differently across the business cycle, I extend the local-projection framework to allow the impulse response to vary with the state of the economy. Following the state-dependent LP literature (e.g., Auerbach and Gorodnichenko, 2012; Ramey and Zubairy, 2018) and the system interpretation of local projections developed in Jordà, 2005, 2009; Plagborg-Møller and Wolf, 2021, I estimate the following state-dependent LP model jointly across all horizons:

$$y_{t+h} = \alpha_h + \beta_h^{\text{Exp}} \text{Shock}_t \, (1 - I_{t-1}) + \beta_h^{\text{Rec}} \text{Shock}_t \, I_{t-1} + \boldsymbol{\gamma}_h' X_{t-1} + \varepsilon_{t+h}, \qquad h = 0, 1, \dots, H, \quad (4)$$

where I_{t-1} is an indicator equal to one when the economy is in a bad state at time $t-1$ and zero otherwise, and X_{t-1} collects lagged controls. The coefficients β_h^{Exp} and β_h^{Rec} trace the impulse-response functions in expansions and recessions, respectively. The state is defined using the unemployment rate relative to a fixed threshold. In the baseline specification, the threshold is the full-sample median unemployment rate of 5.5 percent; Appendix B5 reports results for alternative cutoffs.

Rather than estimating (4) separately for each horizon, I adopt the system local-projection (LP) approach (Jordà, 2009; Montiel Olea and Plagborg-Møller, 2019; Plagborg-Møller and Wolf, 2021) and estimate all horizons jointly by stacking the data. In this formulation, the set of horizon-specific LP equations is treated as a single regression system with horizon fixed effects and horizon-specific shock interactions. The system estimator delivers the same impulse-response coefficients as the conventional horizon-by-horizon LP implementation, but it additionally

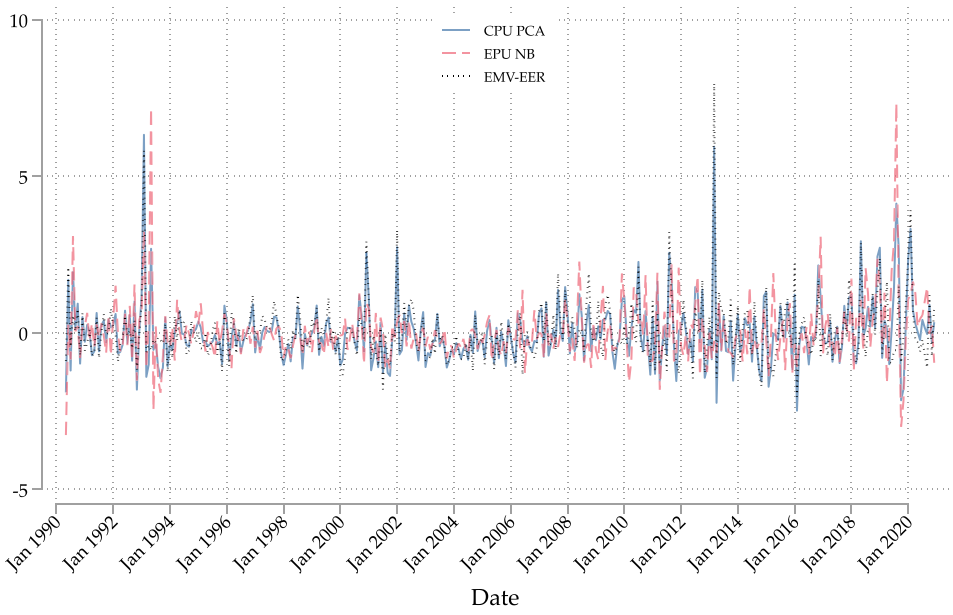

Fig. 1. Standardized CPU shock series.

recovers the full variance–covariance matrix of the impulse-response vector, in the spirit of Jordà (2009). The resulting joint variance–covariance matrix, $\hat{\boldsymbol{\Sigma}}_\beta$ for $\boldsymbol{\beta} = (\beta_0, \ldots, \beta_H)'$, permits valid joint inference across horizons and facilitates formal Wald tests of (i) whether the entire impulse-response function is statistically different from zero and (ii) whether impulse responses differ across economic states. Standard errors are clustered at the time level to accommodate the moving-average structure induced by overlapping forecast horizons, yielding heteroskedasticity- and autocorrelation-robust inference (Montiel Olea and Plagborg-Møller, 2021).

A further advantage of the stacked estimator is that the estimation sample is held fixed across all horizons. This stands in contrast to the standard horizon-by-horizon LP approach, in which the effective sample size declines mechanically at longer horizons as observations near the end of the sample are lost. The fixed-sample property is particularly important for joint inference, since all horizon-specific coefficients are estimated from an identical set of time periods, ensuring that joint F-tests are not confounded by variation in sample composition across horizons.[3]

The control vector X_{t-1} includes the same set of lagged uncertainty indicators as in the linear specification — lags of the VIX, Economic Policy Uncertainty, and the dependent variable — to ensure that the estimated response to CPU shocks is not confounded by other sources of uncertainty or macroeconomic persistence. Estimating (4) for horizons $h = 0, \ldots, 60$ yields two complete impulse-response functions, one for expansions and one for recessions, which permits a direct statistical assessment of whether the macroeconomic effects of CPU are state dependent.

4. Empirical evidence

This section presents impulse response functions (IRFs) for key macroeconomic and financial variables in response to a standardized innovation in climate and environmental policy uncertainty from the PCA index. Appendix B.2 presents the IRFs for the individual indices as robustness checks.[4] Additionally, to highlight the unique impact of the CPU shock, I benchmark its effects against two established broad measures of uncertainty: the VIX index as a proxy for aggregate financial uncertainty and the general Equity Market Volatility Tracker (Baker et al., 2026) in Appendix A.3.

Fig. 2 illustrates the dynamic effects of a one-standard-deviation innovation in the composite climate-policy-uncertainty index. Both the OLS-based (dashed) and IV-based (solid) estimates closely coincide, confirming that instrumenting the PCA index does not materially change the results. These responses reveal a coherent story of how heightened climate-policy uncertainty propagates through the real economy and financial markets, consistent with the "negative-demand" mechanism emphasized by Baker et al. (2016), and the bank-lending amplification stressed by Basu and Bundick (2017).

The results reveal a broad contractionary transmission where investment falls by approximately 1% and industrial production contracts by a similar magnitude. This real-side weakness is accompanied by a deterioration in labor markets, as the unemployment rate rises by 0.3 percentage points, and a persistent drop in consumption. Financial channels amplify this downturn; business loans contract by around 1.5%, suggesting that heightened uncertainty tightens credit frictions rather than merely inducing voluntary investment delays. In response, the Federal Reserve eases policy by lowering the federal funds rate, while core inflation moderates. These dynamics characterize CPU as a disinflationary negative demand shock with lasting consequences for aggregate activity.

The distinctive signature of CPU emerges when comparing its environmental impact against generic financial uncertainty (see Appendix B.3). While VIX shocks depress activity, they generate no statistically significant change in CO_2 emissions. CPU shocks, conversely, drive an immediate and sustained reduction in carbon emissions. This divergence indicates a targeted transmission channel rather than a general "risk-off" mechanism.

Sectoral analysis confirms this targeted nature. As shown in Fig. 3, fossil-fuel industrial production plunges by about 2% and remains suppressed over the full horizon, a contraction twice as deep as that of the

[3] Appendix B4 reports robustness checks for shorter horizons, since longer horizons may spuriously reject the null of equal responses due to increased estimation uncertainty at distant horizons.

[4] I also assess the EMV-EER tracker over a longer period, up to 2025.

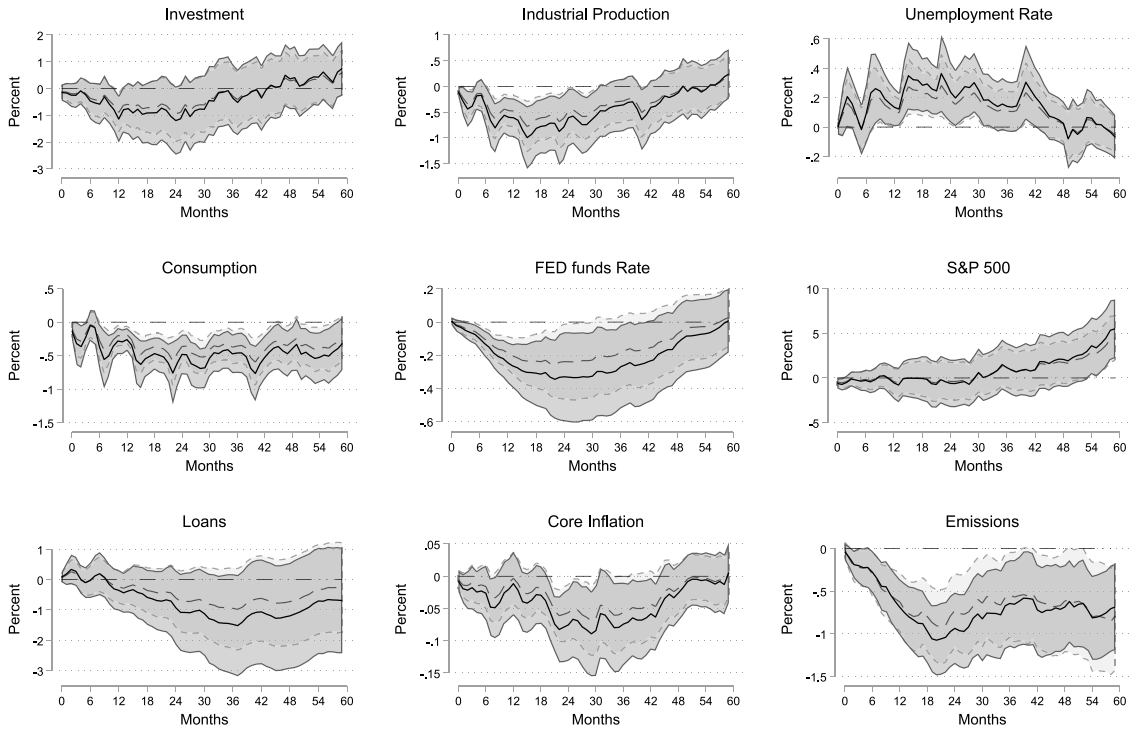

Fig. 2. Impulse Response Functions to 1 sd PCA shock — OLS (dashed) and IV (solid).
Note: 90% CI. In OLS I use the index shock, while in the IV the shock instruments the index.

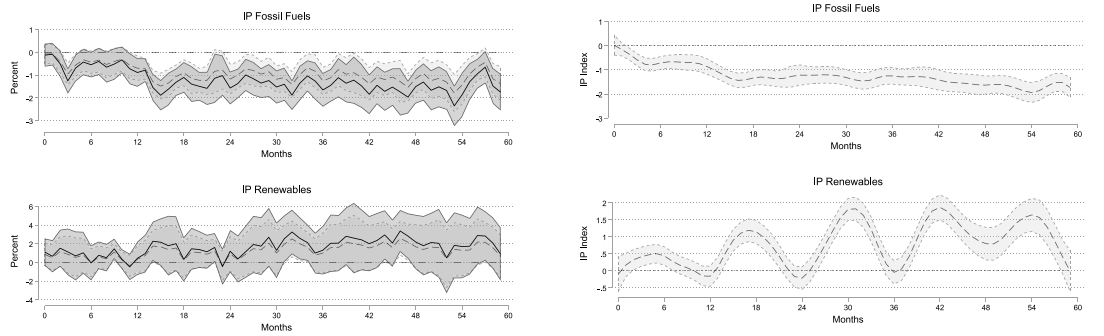

Fig. 3. IP Index IRF to 1 sd PCA shock — Left OLS (dashed) and IV (solid) — Right Smooth LP.

aggregate index. Renewable energy output exhibits an inverse pattern; it remains flat initially but subsequently expands by 1 to 2 percent. This decoupling implies that climate policy uncertainty induces a structural reallocation. Fossil-fuel firms retrench in the face of regulatory ambiguity and financing constraints, while renewable producers absorb the shift in resources. Unlike broad equity market volatility which is sector-neutral, CPU actively reshapes the composition of energy production.

Considering the behavior of total emissions, these sectoral responses point toward a structural shift rather than cyclical weakness. Whereas total industrial output and aggregate emissions both decline on impact under high uncertainty, emissions fall more steeply and remain lower for longer, tracking the fossil-fuel drop rather than the milder contraction of overall IP. Meanwhile, renewables expand, indicating that some of the cooling in aggregate industrial activity is offset by a sustained boost to clean-energy sectors. This differential behavior across fossil and renewable IP confirms that climate-policy uncertainty induces a compositional reallocation away from high-carbon electricity. This asymmetric response differs from the effects of VIX and the Overall Equity Market Volatility Tracker (Baker et al., 2026) shocks, which are sector-neutral and have no differential impact on fossil fuel versus renewable energy production (see Appendix B3).

These patterns are consistent with the mechanisms emphasized in Baker et al. (2016) and Basu and Bundick (2017). In their framework, uncertainty shocks weaken aggregate demand and tighten credit, but they also introduce precautionary incentives and alter relative returns across sectors. I see that here: fossil-fuel firms, facing ambiguous future regulations and financing constraints, cut back sharply. In contrast, renewable producers, whose long-term prospects look more stable under heightened regulatory risk for carbon, attract new investment and expand output. In short, the joint response for fossil and renewable IP supports the interpretation that climate-policy uncertainty not only depresses overall industrial activity but also favors a transition toward low-carbon electricity generation.

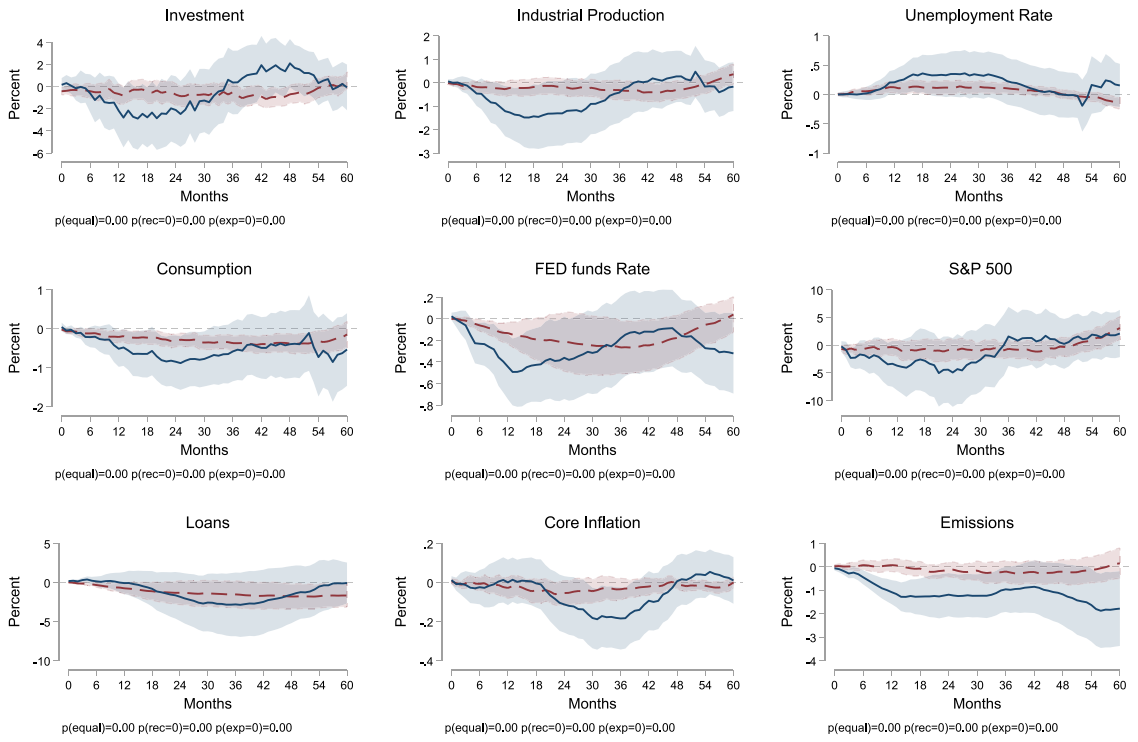

Fig. 4. State-Dependent IRFs to a 1 SD CPU Shock — Low (solid) vs High (dashed) Unemployment.
Notes: Shaded areas: 90% CIs. p-values from joint F-tests across all horizons. SEs clustered by time. (For interpretation of the references to color in this figure legend, the reader is referred to the web version of this article.)

These findings establish that climate policy uncertainty operates as a multi-channel shock that dampens aggregate demand through tighter credit while simultaneously enforcing a green transition in the energy sector. Having identified this reallocation mechanism, the analysis next explores how its strength varies across the business cycle.

4.1. State-dependent impulse response

The unconditional analysis established that Climate Policy Uncertainty (CPU) has a unique, sector-specific footprint. I now investigate the question motivated by this finding: under what macroeconomic conditions is this targeted reallocation channel most potent?

Fig. 4 presents a key empirical finding of this paper. The impact of a CPU shock is contingent on the state of the business cycle, which has a strong reallocation channel toward clean energy, demonstrating a clear asymmetry in its potency.

During Expansions (Low Unemployment), a CPU shock acts as a contractionary force. It triggers a decline in investment, which falls by almost 2% at its trough. This decline in capital spending spreads quickly to the rest of the economy: industrial production contracts sharply, and the unemployment rate rises by approximately 0.4 percentage points. Financial conditions tighten in response, with bank lending falling (although not statistically significant). The Federal Reserve is forced to pursue a strong easing cycle, cutting the policy rate by nearly 40 basis points to counteract the negative demand shock.

During Recessions (High Unemployment), the red lines illustrate a different reality. In periods when the economy is already weak, the same CPU shock behaves almost like a non-event. The impulse responses for investment, economic activity, lending, consumption, and unemployment are almost flat but still mildly negative. The small drop in the first periods of the Industrial Production Index translates into a mild decrease in emissions, but it is not as sharp in the expansion regime.

This asymmetric potency is a characteristic of CPU. While standard financial uncertainty, proxied by the VIX or the General Equity Market Volatility Tracker, is also damaging in expansions, it continues to show negative effects during recessions (see Appendix B3). In some cases, the drop in real variables is even greater in magnitude during recessions than in expansions. By contrast, the impact of CPU in recessions is weaker. This suggests that a sectoral reallocation channel, a unique feature of CPU, is effectively "switched off" when the economy is weak. Neither of the two general uncertainty shocks shows this state-dependent feature or the carbon footprint reallocation channel, as the responses of the sectoral energy Industrial Production index remain muted and similar across episodes of high and low unemployment.

The economic intuition for this asymmetry draws on the "option to wait" framework (Bloom, 2009), though the mechanism differs from standard uncertainty shocks in important ways. During expansions, firms are actively investing and expanding, making them sensitive to signals about the future viability of carbon-intensive capital. A CPU shock disrupts investment plans by altering the relative attractiveness of brown versus green assets, triggering postponement or cancellation of projects and initiating sectoral reallocation. During recessions, investment is already depressed due to weak demand and tight credit conditions, limiting the scope for further contraction through the uncertainty channel.

The CPU shocks have a milder impact during recessions. Indeed, the joint F-tests reject the null that recession-state IRFs equal zero for most variables. Rather, the effects are significantly muted relative to expansionary periods. This pattern is consistent with a partial attenuation of the transmission mechanism: while the collateral channel remains operative during downturns, its marginal impact is diminished when

credit conditions are already constrained and investment demand is weak.

The comparison with broad uncertainty measures reinforces this interpretation. As shown in the robustness analysis, VIX and Overall EMV Tracker shocks also exhibit state-dependence, but with a qualitatively different pattern: their contractionary effects are actually larger during high unemployment episodes, consistent with credit and precautionary savings channels that amplify during downturns. The fact that CPU shocks display the opposite asymmetry, with stronger effects during expansions, suggests that their transmission operates predominantly through sectoral reallocation rather than aggregate demand contraction. During recessions, the reallocation channel loses strength because firms lack the capacity to redirect investment toward cleaner technologies, even as the collateral channel continues to exert some residual effect. This distinct pattern of state-dependence provides further evidence that climate policy uncertainty represents a structurally different source of macroeconomic fluctuations, one whose primary transmission mechanism is tied to the composition rather than the level of economic activity.

The sectoral energy production data in Fig. 5 provide direct and compelling evidence for this mechanism. In the expansionary state (blue), the CPU shock causes a decline in fossil fuel production, while leaving renewables unaffected. This is the sectoral reallocation channel in action: the shock's entire macroeconomic impact is driven by a targeted halt in carbon-intensive activity. In the recessionary state (red), however, the shock has no discernible impact on either energy source. This confirms that the sectoral reallocation mechanism is the primary channel of transmission and that it is only operative during economic expansions.

The contrast with broad uncertainty measures is instructive. While the VIX and the overall EMV tracker also exhibit statistically significant state-dependence over the 60-month horizon, their transmission mechanisms differ qualitatively from those of CPU shocks. For these general uncertainty indices, the negative effects on real and financial variables are larger during high unemployment episodes, which is the opposite pattern from CPU shocks. This divergence highlights that climate policy uncertainty represents a distinct source of macroeconomic fluctuations, operating through sector-specific reallocation channels rather than solely through aggregate demand contraction.

These state-dependent results are robust to alternative unemployment cutoffs. Appendix B.5 presents impulse responses using five different thresholds: the median unemployment rate over 1985–2025 (5.4%), the median over 1990–2025 (5.5%), the mean over 1985–2025 (5.75%), the mean over 1990–2020 (5.91%), and the 6.5% cutoff used by Ramey and Zubairy (2018). Across all specifications, the core finding remains unchanged: CPU shocks have significantly larger effects during expansions than during recessions.

5. Model

The empirical analysis shows that climate policy uncertainty (CPU) behaves as a distinct macroeconomic shock with a strongly state-dependent footprint: its contractionary effects arise in expansions and are negligible in recessions. The evidence points to a sectoral reallocation channel in which uncertainty disproportionately disrupts carbon-intensive activity when the economy is operating strongly.

To interpret these regularities, I develop a two-sector New Keynesian DSGE model with green and brown production. The model combines three ingredients. First, a two-sector structure allows CPU to reallocate activity away from the brown sector and toward cleaner production. Second, financial intermediation frictions in the spirit of Gertler and Karadi (2011) amplify shocks through bank balance sheets, credit supply, and risk premia, particularly when the valuation of brown capital becomes more uncertain. Third, households have Epstein–Zin preferences, which separate risk aversion from intertemporal substitution and generate precautionary responses to second-moment shocks (Basu and Bundick, 2017). The model extends Diluiso et al. (2021) and related work by integrating sectoral reallocation and financial amplification under uncertainty in a framework suitable for state-dependent dynamics.

5.1. Households

A representative household values consumption c_t and leisure $1 - L_t$ using Epstein–Zin recursive preferences (Epstein and Zin, 2013). Following Gertler and Karadi (2011), a fraction $1 - f$ of household members are workers and a fraction f are bankers; individuals transition across occupations, but aggregate shares remain constant. The household's continuation value is

$$V_t = \left((1-\beta)\left(c_t^{\omega}\left(1-L_t\right)^{1-\omega}\right)^{1-\rho} + \beta\left[\mathbb{E}_t(V_{t+1}^{1-\sigma})\right]^{\frac{1-\rho}{1-\sigma}}\right)^{\frac{1}{1-\rho}}. \tag{5}$$

Here ω is the consumption weight, β the discount factor, σ risk aversion, and ψ the elasticity of intertemporal substitution with $\rho = 1/\psi$. Labor is a CES composite,

$$L_t = \left(L_{b,t}^{1+\rho_l} + L_{g,t}^{1+\rho_l}\right)^{\frac{1}{1+\rho_l}},$$

where ρ_l governs substitution across sectoral labor inputs.

The budget constraint is

$$c_t + D_{t+1} = w_{b,t}L_{b,t} + w_{g,t}L_{g,t} + T_t + R_t D_t + \Pi_{t,g} + \Pi_{t,b} + \Phi_t, \tag{6}$$

where D_{t+1} are one-period deposits (or bonds), R_t is the gross return, $\Pi_{t,k}$ are profits from non-financial firms, Φ_t are transfers associated with banker entry, and T_t are lump-sum taxes/transfers. The optimality conditions imply standard sectoral labor supply conditions and an Euler equation with stochastic discount factor

$$M_{t,t+1} = \beta\frac{C_t}{C_{t+1}}\frac{\left(C_{t+1}^{\omega}(1-L_{t+1})^{1-\omega}\right)^{1-\rho}}{\left(C_t^{\omega}(1-L_t)^{1-\omega}\right)^{1-\rho}}\left(\frac{V_{t+1}^{1-\sigma}}{\mathbb{E}_t\left(V_{t+1}\right)^{1-\sigma}}\right)^{\frac{\rho-\sigma}{1-\sigma}}, \qquad \mathbb{E}_t\left[M_{t,t+1}R_{t+1}\right] = 1.$$

5.2. Final goods

A competitive final-good firm aggregates differentiated intermediate inputs:

$$Y_t = \left[\int_0^1 y_t(i)^{\frac{\epsilon-1}{\epsilon}}\,di\right]^{\frac{\epsilon}{\epsilon-1}}, \tag{7}$$

implying demand $y_t(i) = Y_t\left(\frac{p_t(i)}{P_t}\right)^{-\epsilon}$.

5.3. Intermediate goods and price setting

Each intermediate firm produces a differentiated input using a CES bundle of green and brown goods:

$$y_t(i) = \left[(1-\zeta)^{\frac{1}{\gamma}}(y_{g,t}(i))^{\frac{\gamma-1}{\gamma}} + \zeta^{\frac{1}{\gamma}}(y_{b,t}(i))^{\frac{\gamma-1}{\gamma}}\right], \tag{8}$$

where ζ is the brown share and γ is the elasticity of substitution. Cost minimization yields input demands

$$y_{g,t} = (1-\zeta)\left(\frac{p_{g,t}}{MC_t}\right)^{-\gamma}y_t(i), \qquad y_{b,t} = \zeta\left(\frac{p_{b,t}}{MC_t}\right)^{-\gamma}y_t(i), \tag{9}$$

with marginal cost

$$MC_t = \left[(1-\zeta)p_{g,t}^{1-\gamma} + \zeta p_{b,t}^{1-\gamma}\right]^{\frac{1}{1-\gamma}}.$$

Prices are set under Rotemberg adjustment costs, delivering a nonlinear Phillips curve:

$$\pi_t(\pi_t - \bar{\pi}) = \mathbb{E}_t\left[M_{t,t+1}\pi_{t+1}(\pi_{t+1} - \bar{\pi})\frac{y_{t+1}}{y_t}\right] + \frac{\epsilon}{\kappa_P}\left(MC_t - \frac{\epsilon-1}{\epsilon}\right). \tag{10}$$

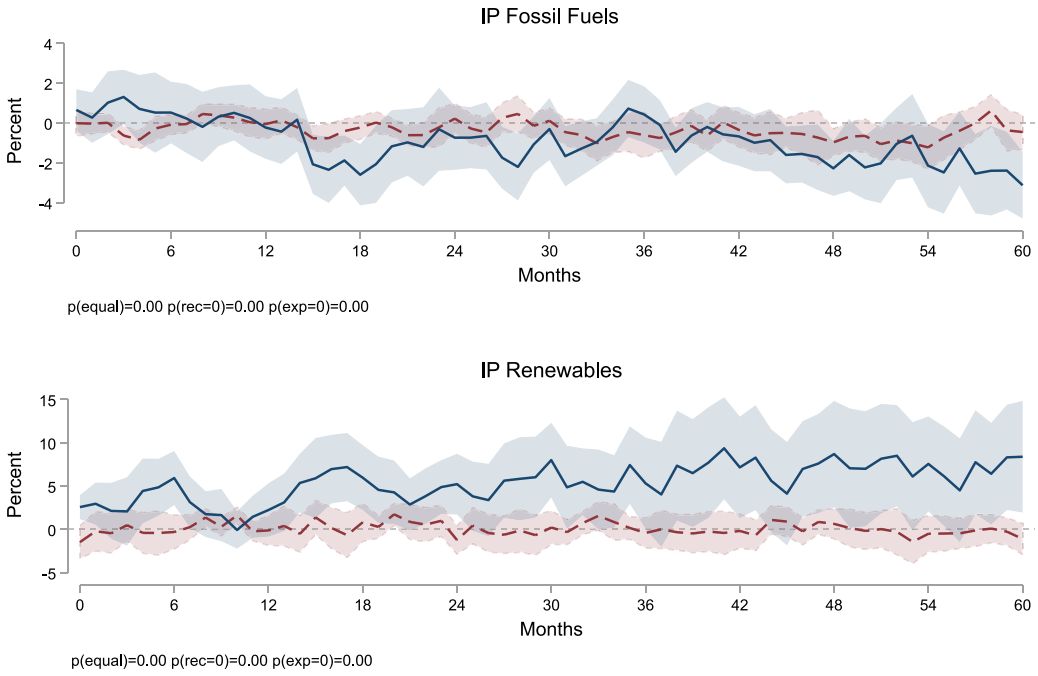

Fig. 5. State-Dependent IRFs for Energy IP — Low (solid) vs High (dashed) Unemployment.
Notes: Shaded areas: 90% CIs. p-values from joint F-tests across all horizons. SEs clustered by time. (For interpretation of the references to color in this figure legend, the reader is referred to the web version of this article.)

5.4. Green and brown production, damages, and emissions

Sectoral output is produced via Cobb–Douglas technology:

$$y_{k,t} = A_t(\xi_{k,t}K_{t-1,k})^{\alpha}L_{t,k}^{1-\alpha}. \tag{11}$$

Aggregate productivity is reduced by pollution damages:

$$A_t = \left(1 - (D_0 + D_1X_t + D_2X_t^2)a\right), \tag{12}$$

where X_t is the pollution stock and a is an AR(1) TFP shock. Only the brown sector emits:

$$X_t = (1-\delta_x)X_{t-1} + e_t + e^*, \qquad e_t = y_{b,t}. \tag{13}$$

Brown firms face a carbon tax τ_t and finance capital via bonds, while green firms are untaxed. The brown firm's optimality conditions reflect the tax wedge in factor demands; the green firm's conditions are analogous without τ_t.

5.5. Capital producers

Capital producers transform final output into sector-specific capital subject to adjustment costs:

$$\max\ \mathbb{E}_0 \sum_{t=0}^{\infty} M_{0,t} \sum_{k=b,g} \left[q_{k,t}k_{k,t} - (1-\delta)q_{k,t}k_{k,t-1} - i_{k,t}\right]$$

$$\text{s.t.}\ \ k_{k,t} = (1-\delta)k_{k,t-1} + \left[1 - \frac{\kappa_I}{2}\left(\frac{i_{k,t}}{i_{k,t-1}} - 1\right)^2\right]i_{k,t},$$

implying the standard Tobin's q condition with investment adjustment costs (FOC omitted for brevity).

5.6. Financial intermediaries

Banks raise deposits and allocate credit across green and brown firms. Their balance sheet is

$$b_{g,t}^f + b_{b,t}^f = NW_t + D_t, \tag{14}$$

where NW_t is net worth. To capture sluggish portfolio reallocation, banks pay a quadratic cost when deviating from a steady-state green share b^*, which affects net-worth dynamics:

$$NW_t = r_{g,t}b_{g,t-1}^f + r_{b,t}b_{b,t-1}^f - \frac{r_{t-1}}{\pi_t}D_{t-1} - \frac{\kappa_F}{2}NW_{t-1}\left(\frac{b_{g,t-1}^f}{b_{t-1}^f} - b^*\right)^2. \tag{15}$$

Following Gertler and Karadi (2011), an agency constraint limits leverage:

$$V_t^f \geq \theta_t(b_{g,t}^f + b_{b,t}^f), \tag{16}$$

and the constraint is assumed to bind in equilibrium. The resulting leverage and portfolio conditions (reported above) generate a financial accelerator: when bank equity is low, spreads rise and lending contracts, amplifying shocks. This mechanism is central for interpreting how uncertainty about brown asset values translates into macroeconomic responses that vary with financial conditions.

5.7. Monetary policy and market clearing

Monetary policy follows a Taylor rule with interest rate smoothing:

$$\frac{r_t}{\bar{r}} = \left(\frac{r_{t-1}}{\bar{r}}\right)^{\rho_r}\left[\left(\frac{\pi_t}{\bar{\pi}}\right)^{\rho_\pi}\left(\frac{Y_t}{Y^*}\right)^{\rho_y}\right]^{1-\rho_r}e_t^{m_t}. \tag{17}$$

Final-good market clearing is

$$y_t = c_t + I_t + \frac{\kappa_F}{2}NW_{t-1}\left(\frac{b_{g,t-1}^f}{b_{t-1}^f} - b^*\right)^2 + \frac{\kappa_p}{2}\left(\frac{p_t(i)}{p_{t-1}(i)} - \bar{\pi}\right)^2 y_t. \tag{18}$$

5.8. Uncertainty shocks and calibration

CPU enters the model through second-moment shocks. I consider two alternative channels: (i) volatility in brown-sector capital quality, capturing uncertainty about the valuation of carbon-intensive capital, and (ii) volatility in the carbon tax, capturing uncertainty about

Table 1
GARCH(1,1) Estimates for CPU.

Parameter	Estimate	Std. Error
ρ_{CPU} (AR coefficient)	0.7810	(0.1615)
ω (GARCH constant)	0.0017	(0.0011)
α (ARCH term)	0.2470	(0.2952)
β (GARCH term)	0.3279	(0.3974)

Notes: Robust standard errors in parentheses.

Table 2
Calibrated stochastic volatility parameters.

Parameter	Description	Value
ρ_σ	Persistence of volatility	0.5749
$\bar{\sigma}$	Steady-state volatility	0.06302
σ_σ	Volatility of volatility	0.0443

Notes: Parameters recovered from Table 1.

policy stringency. In both cases, the shock follows an AR(1) with time-varying volatility, following Fernández-Villaverde and Guerrón-Quintana (2020), for the Brown Capital Quality shock is:

$$\xi_{b,t} = \rho_\xi \xi_{b,t-1} + \sigma_{\xi,t}\epsilon_{\xi,t}, \quad \sigma_{\xi,t} = (1-\rho_\sigma)\bar{\sigma} + \rho_\sigma \sigma_{\xi,t-1} + \sigma_\sigma \eta_{\xi,t} \tag{19}$$

and for the carbon-tax:

$$\tau_t = \rho_\xi \tau_{t-1} + \sigma_{\tau,t}\epsilon_{\tau,t}, \quad \sigma_{\tau,t} = (1-\rho_\sigma)\bar{\sigma} + \rho_\sigma \sigma_{\tau,t-1} + \sigma_\sigma \eta_{\tau,t} \tag{20}$$

I discipline $(\rho_\sigma, \bar{\sigma}, \sigma_\sigma)$ using an AR(1)-GARCH(1,1) estimated on the demeaned CPU index:

$$C\tilde{P}U_t = \rho_{CPU} C\tilde{P}U_{t-1} + \varepsilon_t, \quad \varepsilon_t \sim N(0, h_t),$$
$$h_t = \omega + \alpha \varepsilon_{t-1}^2 + \beta h_{t-1},$$

Then, I map GARCH estimates into stochastic-volatility parameters using:

$$\rho_\sigma = \alpha + \beta, \qquad \bar{\sigma} = \sqrt{\frac{\omega}{1-(\alpha+\beta)}}, \qquad \sigma_\sigma = \sqrt{2\alpha}\,\bar{\sigma}.$$

Table 1 reports the GARCH estimates and Table 2 reports the implied volatility parameters. Importantly, both the capital-quality and carbon-tax specifications use the same volatility calibration so that differences in simulated outcomes reflect transmission mechanisms rather than assumed volatility dynamics.

To assess which channel better matches the empirical evidence, I simulate the model under the two specifications: CPU operating solely through capital-quality uncertainty in the brown sector, and CPU operating solely through carbon-tax uncertainty. Both use the parameters in Table 2.

5.9. Calibration

The model is calibrated to match key features of the U.S. economy at a quarterly frequency. The parameterization draws upon established values from the literature, particularly Ferrari and Nispi Landi (2024), Barrage (2020), Carattini et al. (2023), and Gertler and Karadi (2011). Table 3 summarizes the baseline parameter values, with comprehensive details on the calibration strategy, especially for targeted parameters, provided in Appendix B.

Several standard macroeconomic parameters are adopted from the Smets and Wouters (2007). The discount factor β is set to achieve a steady-state annualized real interest rate of 2% on public debt. Additionally, θ is calibrated to yield a steady-state total bank leverage ratio of 6, and ι is chosen to match an annualized steady-state corporate spread of 2%. The price stickiness parameter κ_p corresponds to a Calvo probability of 0.82.

Household preference parameters are informed by Barrage (2020) for the consumption utility weight. The medium risk aversion parameter implies that uncertainty matters, but it is lower than in other papers that use Epstein–Zin utility functions, as in Basu and Bundick (2017).

For the environmental block parameters, I follow the methodology described in Gibson and Heutel (2023) and implemented by Ferrari and Nispi Landi (2024) (see Table 4).

Finally, concerning the substitutability between energy inputs, I adopt $\gamma = 2$ from Carattini et al. (2023), indicating imperfect substitution between green and brown goods. Consistent with Giovanardi et al. (2023), the weight assigned to the brown good in the compound is $\zeta = 0.8$.[5]

5.10. Solution method

The objective of this analysis is to examine the effects of an increase in the second moment of two critical shock processes: the brown capital quality shock and the carbon tax shock. Capturing the impulse responses to such second-moment shocks requires employing at least a third-order approximation of the model's policy functions, as lower-order approximations fail to capture the effects of volatility on decision rules (Fernández-Villaverde et al., 2015; Basu and Bundick, 2017). I solve the model using Dynare, which computes rational expectations solutions via a third-order Taylor series expansion around the deterministic steady state with pruning to prevent explosive sample paths.

The impulse response functions are generated through a simulation procedure that accounts for the nonlinear nature of uncertainty shocks. First, I simulate the model for a burn-in period (100) without shocks to obtain the stochastic steady state, an equilibrium that incorporates the precautionary effects of background uncertainty. This stochastic steady state serves as the appropriate baseline, since agents in the model anticipate the possibility of future volatility fluctuations even in the absence of current shocks.

Second, I introduce a one-standard-deviation shock to the volatility process ($\sigma_{\xi,t}$ or $\sigma_{\tau,t}$) immediately following the burn-in phase. The impulse responses are computed as the difference between the shocked and baseline paths, averaged over a large number of simulations to eliminate sampling variation. This generalized impulse response methodology, standard in the literature on uncertainty shocks, ensures that the reported dynamics reflect the causal effect of increased volatility rather than the realization of any particular sequence of first-moment innovations.

To compare the two transmission channels, I simulate the model under each specification separately. In the capital quality specification, a shock to $\sigma_{\xi,t}$ increases uncertainty about the future productivity of brown-sector capital, triggering the financial amplification mechanism. In the carbon tax specification, a shock to $\sigma_{\tau,t}$ increases uncertainty about future emissions costs, affecting expected profits and abatement decisions. Both specifications use identical volatility parameters calibrated from the estimation on the empirical CPU index, ensuring that the comparison isolates differences in transmission mechanisms rather than differences in shock properties.

The model-implied IRFs are then compared to the empirical estimates from local projections. This comparison provides a transparent assessment of which channel better explains the observed macroeconomic response to climate policy uncertainty, without relying on formal estimation that could obscure the source of identification.

[5] Also, we can interpret this as the share of Renewable Energy use in the US economy, which is about% according to the U.S. Energy Information Administration.

Table 3
Macroeconomic and household parameters.

Parameter	Description	Value	Source
β	Discount factor	0.995	Standard
α	Capital share in production	0.33	Standard
ψ	Intertemporal elasticity of substitution	1.5	Standard
σ	Risk aversion coefficient	10	Moderate risk aversion
ω	Weight of consumption in utility	0.32	Barrage (2020)
δ	Capital depreciation rate	2.5%	Standard
ρ_l	Elasticity of substitution for labor hours	1	Carattini et al. (2023)
γ	Elasticity of substitution for brown and green goods	2	Carattini et al. (2023)
ζ	Weight of brown goods in consumption	0.8	Giovanardi et al. (2023)
κ_p	Price adjustment cost	70	Match Calvo = 0.82
$\bar{\pi}$	Target inflation rate	1.005	2% Fed Target
κ_I	Investment adjustment cost	20.78	To match inv. volatility
$\bar{r}$	Steady-state nominal interest rate	1.01	Standard
ρ_r	Interest rate smoothing parameter in Taylor rule	0.80	Smets and Wouters (2007)
ρ_π	Inflation responsiveness in Taylor rule	2	Smets and Wouters (2007)
ρ_y	Output gap responsiveness in Taylor rule	0.03	Smets and Wouters (2007)
ρ_a	Persistence of technology shock	0.95	Smets and Wouters (2007)
$\rho_{\bar{\xi}}$	Persistence of capital quality shock	0.66	Gertler and Karadi (2011)

Table 4
Environmental and financial sector parameters.

Parameter	Description	Value	Source
D_0	Constant term in damage function	−0.0076	Gibson and Heutel (2023)
D_1	Linear term in damage function	9.0182×10^{-7}	Gibson and Heutel (2023)
D_2	Quadratic term in damage function	1.2013×10^{-10}	Gibson and Heutel (2023)
δ_x	Pollution decay rate	0.0035	Gibson and Heutel (2023)
e^{row}	Constant emissions level	25.11	Gibson and Heutel (2023)
κ_F	Bank portfolio adjustment cost	3	Ferrari and Nispi Landi (2024)
θ	Divertible portion of assets	0.4474	Match $lev_{ss} = 6$
χ	Banks' survival probability	0.972	Gertler and Karadi (2011)
ι	Wealth share for new banks	0.002	Gertler and Karadi (2011)

6. Quantitative results

This section evaluates the model's ability to reproduce the empirical impulse responses by simulating two distinct second-moment shocks: volatility in the quality of brown capital ($\sigma_{\bar{\xi}}$) and volatility in the carbon tax rate (σ_τ). Fig. 6 overlays these theoretical responses against the empirical estimates, which display a recessionary pattern characterized by falling output, consumption, and investment, rising unemployment, and a persistent easing of monetary policy. The brown capital quality volatility shock (black solid line) closely tracks the empirical dynamics. It generates an immediate and persistent contraction in aggregate activity, with output declining by 0.5% to 0.8% and investment falling by 2% at the trough (quarters 6 to 8). Consistent with the data, the model produces a hump-shaped rise in unemployment and a policy rate cut of approximately 0.2 to 0.3 percentage points. In contrast, the carbon tax volatility shock (blue dashed line) fails to match the empirical regularity. It produces negligible or slightly positive effects on aggregate activity and investment, behaving more like a reallocation disturbance than the broad contractionary shock observed in the data.

The sectoral decomposition in Fig. 7 further distinguishes the two mechanisms. Under the capital quality shock, brown investment plunges by 8% while brown output falls by 0.6%, driving the persistent decline in emissions of roughly 0.8% observed empirically. Green activity initially softens due to negative aggregate demand spillovers before recovering gradually. This matches the "brown recession" evident in the local projections. Conversely, the tax volatility shock generates a counterfactual "green boom" where renewable investment rises immediately while brown capital remains stable. While this aligns with findings that policy news can stimulate clean investment (Noailly et al., 2024, 2022), it conflicts with the aggregate downturn documented here and in related studies (Palikhe et al., 2024).

These results identify the transmission mechanism. The success of the capital quality specification implies that CPU operates as a shock to the pledgeability of brown assets rather than merely the variance of tax rates. When uncertainty compresses Tobin's q for carbon-intensive capital, it tightens borrowing constraints and triggers the financial amplification channel emphasized by Gilchrist et al. (2014). With nominal rigidities, this credit tightening translates into a broad demand-driven contraction (Basu and Bundick, 2017; Bloom et al., 2018). The resulting fall in fossil fuel activity explains the decline in emissions (Gavriilidis, 2021). By acting as a hit to collateral values, the shock forces a deleveraging that generates the comovement in output, investment, and credit spread widening that the tax volatility channel cannot replicate. This financial accelerator mechanism provides a structural rationale for the state-dependent effects documented in the empirical section, as the shock is most potent when collateral constraints bind, and credit is essential for investment.

6.1. Model mechanisms

6.1.1. The transmission channel: Flow risk vs. Stock risk

A central question is whether Climate Policy Uncertainty is best modeled as volatility in the carbon tax or in the valuation of brown capital. I find that only the capital quality volatility channel can reproduce the empirical regularities—specifically, the sharp tightening of credit conditions and the reallocation of investment. The intuition relies on the distinction between "flow risk" and "stock risk." Carbon tax volatility ($\sigma_{\tau,t}$) acts as flow risk: it increases the variance of future operating costs. While this generates precautionary behavior, the impact is smoothed intertemporally and fails to trigger the sharp asset devaluation required to tighten collateral constraints. In contrast, capital quality volatility ($\sigma_{\bar{\xi},t}$) represents stock risk. It directly impairs the pledgeable value of brown assets ($q_{b,t} K_{b,t}$), which serve as collateral for the banking sector. Because the financial intermediary's leverage constraint is highly sensitive to the value of its assets, this shock forces immediate deleveraging. This "financial accelerator" generates

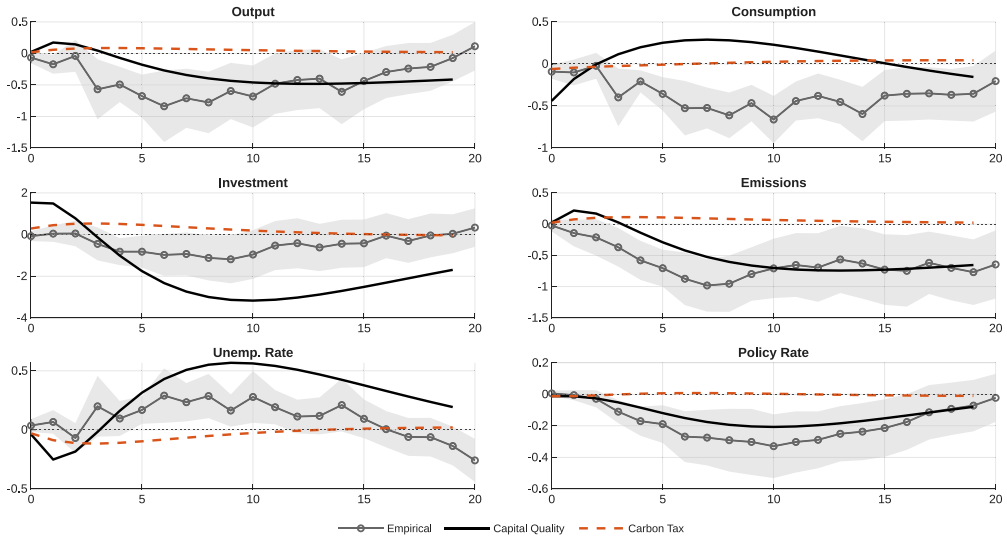

Fig. 6. Empirical and Theoretical IRF: Key Outcome Variables.
Percent deviations from the stochastic steady state; horizontal axis in quarters. Gray circles show empirical point estimates with 90% CI. (For interpretation of the references to color in this figure legend, the reader is referred to the web version of this article.)

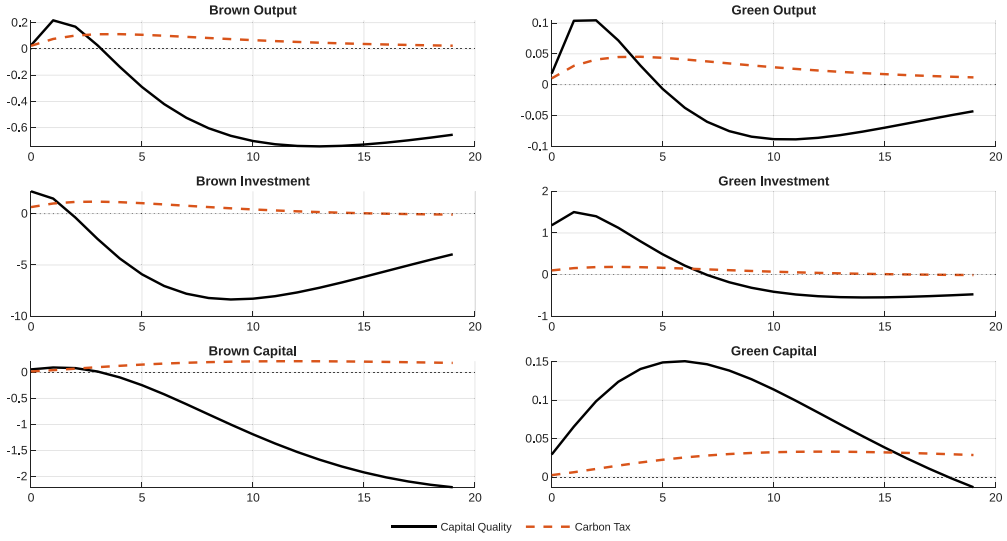

Fig. 7. Theoretical IRF: Sectoral Variables.
Percent deviations from the stochastic steady state; horizontal axis in quarters. Gray circles show empirical point estimates with 90% CI. (For interpretation of the references to color in this figure legend, the reader is referred to the web version of this article.)

the widening spreads and aggregate contraction observed in the data, confirming that CPU operates primarily as a shock to asset values (transition risk) rather than merely statutory costs. See Appendix C4 for a detailed discussion.

6.1.2. *The role of frictions*

To quantify the role of model features, I compare the baseline against counterfactuals with flexible prices and frictionless financial markets (see Appendix C5 for detailed impulse responses). The analysis reveals that financial frictions are the primary amplifier, while nominal rigidities generate the necessary aggregate comovement. Without financial frictions, the shock operates as a relative price disturbance: brown investment falls, but the economy recovers quickly, and monetary policy tightens rather than eases. When financial frictions are present, but prices are flexible, the credit wedge widens, but the real effects are dampened by rapid price adjustments. Consequently, both frictions are necessary to replicate the "demand-like" contraction — where output, investment, and inflation fall simultaneously — observed in the empirical local projections.

6.1.3. *Role of Epstein–Zin preferences*

The choice of Epstein–Zin preferences is essential for matching both asset pricing moments and real quantity dynamics simultaneously. Standard CRRA preferences create a rigid link between risk aversion (σ) and the elasticity of intertemporal substitution ($\psi = 1/\sigma$). As detailed in Appendix C6, this creates an untenable trade-off. Calibrating CRRA to match the high risk premia and credit spreads required for the financial channel ($\sigma \approx 10$) implies an unrealistically low IES, resulting

in explosive volatility in consumption and investment. Conversely, calibrating to match smooth real quantities ($\psi \approx 1.5$) implies low risk aversion, which shuts down the financial accelerator. Epstein–Zin preferences resolve this by decoupling the two parameters, allowing the model to generate the necessary asset price volatility to activate the collateral constraint without inducing counterfactual volatility in real aggregates.

6.1.4. Comparison with aggregate uncertainty

Finally, I distinguish CPU from standard aggregate uncertainty (TFP volatility). While TFP uncertainty depresses activity in both sectors symmetrically, CPU generates a distinct sectoral reallocation. In the model, greater uncertainty about brown capital quality leads banks to rebalance their portfolios, reducing brown lending while increasing green lending (see Appendix C7). This asymmetry — a "brown recession" accompanied by a "green boom" — is a unique signature of transition risk that standard aggregate uncertainty shocks fail to capture.

7. Conclusion and policy implications

This paper shows that Climate Policy Uncertainty (CPU) is a distinct source of macroeconomic instability with a unique state-dependent footprint. Using local projections on U.S. data and a two-sector New Keynesian DSGE model, I show that CPU shocks operate primarily as financial "reallocation shocks" rather than generic uncertainty disturbances. Empirically, CPU exerts a contractionary drag on investment and credit that is concentrated in economic expansions, while having statistically negligible effects during recessions. This asymmetry distinguishes climate transition risk from standard aggregate uncertainty (e.g., VIX), which typically intensifies during downturns.

The theoretical analysis identifies the transmission mechanism driving this result: uncertainty regarding the future value of carbon-intensive capital (stock risk) dominates uncertainty regarding carbon taxes (flow risk). When policy ambiguity undermines the pledgeable value of brown assets, it triggers a financial accelerator mechanism. The resulting devaluation of collateral tightens bank balance sheets and widens credit spreads, propagating the shock through the economy. This channel is most potent during expansions, when leverage constraints bind, and credit is actively flowing.

These findings carry three specific implications for the design of climate and financial policy. The strong state-dependence documented here suggests a difficult trade-off regarding the timing of climate reforms. The empirical results show that expansions are the only periods in which CPU shocks successfully trigger sectoral reallocation, shifting output from brown to green sectors. However, expansions are also when the aggregate costs of these shocks — in terms of lost output and investment — are highest. Conversely, while recessions minimize the aggregate disruption of policy shocks, they also fail to generate the desired "greening" of the economy. This implies that a pure countercyclical strategy, such as delaying reforms until downturns to preserve stability, might inadvertently stall the transition. Future research should formally quantify this welfare trade-off between allocative efficiency and short-run stabilization.

Because the transmission mechanism relies on the collateral channel, transition risk effectively becomes systemic risk. Since brown assets serve as collateral for the broader banking system, ambiguity about their future value drags on aggregate credit provision, extending well beyond the fossil fuel sector. This structural linkage implies that financial regulators should incorporate climate policy uncertainty into prudential frameworks, particularly through stress tests that model the sudden repricing of carbon-intensive collateral rather than just climate physical risks.

Thus, policy credibility emerges as a crucial tool for financial stability. The model shows that the macroeconomic effects of CPU stems from the volatility of asset values rather than the level of the tax itself. Policymakers can therefore mitigate transition costs by reducing the "noise" around implementation; credible long-term commitments, clear phase-in schedules, and predictable regulatory frameworks can anchor asset valuations and prevent the sharp tightening of financial conditions observed in the data. While this mechanism — the financial amplification of stranded asset risk — is analyzed here within the U.S. economy, it is likely relevant for other developed economies undergoing green transitions. Future work should extend this framework to open economy settings to understand how cross-border climate policy spillovers interact with global financial cycles.

Declaration of Generative AI and AI-assisted technologies in the writing process

During the preparation of this work, the author used ChatGPT 5.2 in order to improve the readability, grammatical accuracy, and flow of the text. After using this tool, the author reviewed and edited the content as needed and take full responsibility for the content of the published article.

Declaration of competing interest

The authors declare that they have no known competing financial interests or personal relationships that could have appeared to influence the work reported in this paper.

Appendix A. Supplementary data

Supplementary material related to this article can be found online at https://doi.org/10.1016/j.econmod.2026.107523.

Data availability

Data and Codes available at Mendeley:

Climate Policy Uncertainty and Macroeconomic Dynamics: Financial Amplification and State-Dependent Effects (Original data) (Mendeley Data)

References

Adetutu, M.O., Odusanya, K.A., Stathopoulou, E., Weyman-Jones, T.G., 2023. Environmental regulation, taxes, and activism. Oxf. Econ. Pap. 75 (2), 460–489.
Auerbach, A.J., Gorodnichenko, Y., 2012. Fiscal multipliers in recession and expansion. In: Fiscal Policy After the Financial Crisis. University of Chicago Press, pp. 63–98.
Baker, S.R., Bloom, N., Davis, S.J., 2016. Measuring economic policy uncertainty. Q. J. Econ. 131 (4), 1593–1636.
Baker, S.R., Bloom, N., Davis, S.J., Kost, K.J., 2026. Policy news and stock market volatility. J. Financ. Econ. 175 (1), 104–187.
Barnichon, R., Brownlees, C., 2019. Impulse response estimation by smooth local projections. Rev. Econ. Stat. 101 (3), 522–530.
Barrage, L., 2020. Optimal dynamic carbon taxes in a climate–economy model with distortionary fiscal policy. Rev. Econ. Stud. 87 (1), 1–39.
Basu, S., Bundick, B., 2017. Uncertainty shocks in a model of effective demand. Econometrica 85 (3), 937–958.
Berestycki, C., Carattini, S., Dechezleprêtre, A., Kruse, T., 2022. Measuring and assessing the effects of climate policy uncertainty. OECD.
Bernanke, B.S., 1983. Irreversibility, uncertainty, and cyclical investment. Q. J. Econ. 98 (1), 85–106.
Bilal, A., Känzig, D., 2024. The macroeconomic impact of climate change: Global vs. local temperature. Natl. Bur. Econ. Res. No. W32450.
Bloom, N., 2009. The impact of uncertainty shocks. Econometrica 77 (3), 623–685.
Bloom, N., Floetotto, M., Jaimovich, N., Saporta-Eksten, I., Terry, S.J., 2018. Really uncertain business cycles. Econometrica 86 (3), 1031–1065.
Caldara, D., Iacoviello, M., 2022. Measuring geopolitical risk. Am. Econ. Rev. 112 (4), 1194–1225.
Caldara, D., Iacoviello, M., Molligo, P., Prestipino, A., Raffo, A., 2020. The economic effects of trade policy uncertainty. J. Monet. Econ. 109, 38–59.
Carattini, S., Heutel, G., Melkadze, G., 2023. Climate policy, financial frictions, and transition risk. Rev. Econ. Dyn. 51, 778–794.

Diluiso, F., Annicchiarico, B., Kalkuhl, M., Minx, J.C., 2021. Climate actions and macro-financial stability: The role of central banks. J. Environ. Econ. Manag. 110, 102548.
Eissa, M.A., Al Refai, H., Chortareas, G., 2024. Climate policy uncertainty, geopolitical risk, oil volatility, and global food price volatility: A time-varying analysis. Econ. Model..
Epstein, L.G., Zin, S.E., 2013. Substitution, risk aversion and the temporal behavior of consumption and asset returns: A theoretical framework. In: Handbook of the Fundamentals of Financial Decision Making: Part I. World Scientific, pp. 207–239.
Fernández-Villaverde, J., Guerrón-Quintana, P.A., 2020. Uncertainty shocks and business cycle research. Rev. Econ. Dyn. 37, S118–S146.
Fernández-Villaverde, J., Guerrón-Quintana, P., Kuester, K., Rubio-Ramírez, J., 2015. Fiscal volatility shocks and economic activity. Am. Econ. Rev. 105 (11), 3352–3384.
Ferrari, A., Nispi Landi, V., 2024. Whatever it takes to save the planet? Central banks and unconventional green policy. Macroecon. Dyn. 28 (2), 299–324.
Fried, S., Novan, K., Peterman, W.B., 2021. The macro effects of climate policy uncertainty. Financ. Econ. Discuss. Ser. 2021 (2021–018).
Gavriilidis, K., 2021. Measuring climate policy uncertainty. Available At SSRN 3847388.
Gertler, M., Karadi, P., 2011. A model of unconventional monetary policy. J. Monet. Econ. 58 (1), 17–34.
Gibson, J., Heutel, G., 2023. Pollution and labor market search externalities over the business cycle. J. Econom. Dynam. Control 151, 104665.
Gilchrist, S., Sim, J.W., Zakrajšek, E., 2014. Uncertainty, financial frictions, and investment dynamics. National Bureau of Economic Research, No. w20038.
Giovanardi, F., Kaldorf, M., Radke, L., Wicknig, F., 2023. The preferential treatment of green bonds. Rev. Econ. Dyn. 51, 657–676.
Hoang, B.T., Benbouzid, N., Mallick, S., Stojanovic, A., 2026. Green loans and firm performance: evidence on signalling and impact investing effects. European Financial Manag. 32 (1), 288–312.
Huang, B., Punzi, M.T., 2024. Macroeconomic impact of environmental policy uncertainty and monetary policy implications. J. Clim. Financ. 7, 100040.
Jordà, Ò., 2005. Estimation and inference of impulse responses by local projections. Am. Econ. Rev. 95 (1), 161–182.
Jordà, Ò., 2009. Simultaneous confidence regions for impulse responses. Rev. Econ. Stat. 91 (3), 629–647.
Jurado, K., Ludvigson, S.C., Ng, S., 2015. Measuring uncertainty. Am. Econ. Rev. 105 (3), 1177–1216.
Khalil, M., Strobel, F., 2023. Capital reallocation under climate policy uncertainty. Number 23/2023 in Discussion Paper. Deutsche Bundesbank.
Monasterolo, I., Mandel, A., Battiston, S., Mazzocchetti, A., Oppermann, K., Coony, J., Stretton, S., Stewart, F., Dunz, N., 2024. The role of green financial sector initiatives in the low-carbon transition: A theory of change. Glob. Environ. Chang. 89, 102915.
Montiel Olea, J.L., Plagborg-Møller, M., 2019. Simultaneous confidence bands: Theory, implementation, and an application to SVARs. J. Appl. Econometrics 34 (1), 1–17.
Montiel Olea, J.L., Plagborg-Møller, M., 2021. Local projection inference is simpler and more robust than you think. Econometrica 89 (4), 1789–1823.
NGFS, 2024. Climate change, the macroeconomy and monetary policy. Technical report, Network for Greening the Financial System.
Noailly, J., Nowzohour, L., Van Den Heuvel, M., 2022. Does environmental policy uncertainty hinder investments towards a low-carbon economy? National Bureau of Economic Research, No. w30361.
Noailly, J., Nowzohour, L., Van Den Heuvel, M., Pla, I., 2024. Heard the news? Environmental policy and clean investments. J. Public Econ. 238, 105190.
Olea, J.L.M., Plagborg-Møller, M., Qian, E., Wolf, C.K., 2025. Local projections or vars? A primer for macroeconomists. National Bureau of Economic Research, No. w33871.
Palikhe, H., Schaur, G., Sims, C., 2024. Environmental policy uncertainty. J. Assoc. Environ. Resour. Econ. 11 (5), 1135–1163.
Paudel, J., 2025. Economic impact of large earthquakes: lessons from residential property values. Oxf. Econ. Pap. 77 (2), 564–583.
Pindyck, R.S., 1986. Irreversible investment, capacity choice, and the value of the firm. National Bureau of Economic Research, No. w1980.
Plagborg-Møller, M., Wolf, C.K., 2021. Local projections and VARs estimate the same impulse responses. Econometrica 89 (2), 955–980.
Ramey, V.A., 2018. Ten years after the financial crisis: What have we learned from the vars? J. Econ. Perspect. 32 (3), 89–114.
Ramey, V.A., Zubairy, S., 2018. Government spending multipliers in good times and in bad: evidence from US historical data. J. Political Econ. 126 (2), 850–901.
Ren, X., Zhang, X., Yan, C., Gozgor, G., 2022. Climate policy uncertainty and firm-level total factor productivity: Evidence from China. Energy Econ. 113, 106209.
Smets, F., Wouters, R., 2007. Shocks and frictions in US business cycles: A Bayesian DSGE approach. Am. Econ. Rev. 97 (3), 586–606.
Tan, X., et al., 2024. Nonlinear hedging climate policy uncertainty: A dynamic mixed copula approach. Econ. Model..
Tenreyro, S., Thwaites, G., 2016. Pushing on a string: US monetary policy is less powerful in recessions. Am. Econ. J.: Macroecon. 8 (4), 43–74.